



# In vivo photolabeling of tumor-infiltrating cells reveals highly regulated egress of T-cell subsets from tumors

Tommaso Torcellan<sup>a,b</sup>, Henry R. Hampton<sup>a,b</sup>, Jacqueline Bailey<sup>a</sup>, Michio Tomura<sup>c</sup>, Robert Brink<sup>a,b</sup>, and Tatyana Chtanova<sup>a,b,1</sup>

<sup>a</sup>Immunology Division, Garvan Institute of Medical Research, Darlinghurst, NSW 2010, Australia; <sup>b</sup>St. Vincent's Clinical School, Faculty of Medicine, University of New South Wales Sydney, Darlinghurst, NSW 2010, Australia; and <sup>c</sup>Laboratory of Immunology, Faculty of Pharmacy, Osaka Ohtani University, Tondabayashi City, Osaka Prefecture 584-8540, Japan

Edited by Ruslan Medzhitov, Yale University School of Medicine, New Haven, CT, and approved April 26, 2017 (received for review November 28, 2016)

Immune therapy is rapidly gaining prominence in the clinic as a major weapon against cancer. Whereas much attention has been focused on the infiltration of tumors by immune cells, the subsequent fate of these infiltrates remains largely unexplored. We therefore established a photoconversion-based model that allowed us to label tumor-infiltrating immune cells and follow their migration. Using this system, we identified a population of tumor-experienced cells that emigrate from primary tumors to draining lymph nodes via afferent lymphatic vessels. Although the majority of tumor-infiltrating cells were myeloid, T cells made up the largest population of tumor-egressing leukocytes. Strikingly, the subset composition of tumor-egressing T cells was greatly skewed compared with those that had infiltrated the tumor and those resident in the draining lymph node. Some T-cell subsets such as CD8<sup>+</sup> T cells emigrated more readily; others including CD4<sup>+</sup>CD8<sup>-</sup> T cells were preferentially retained, suggesting that specific mechanisms guide immune cell egress from tumors. Furthermore, tumor-egressing T cells were more activated and displayed enhanced effector function in comparison with their lymph node counterparts. Finally, we demonstrated that tumor-infiltrating T cells migrate to distant secondary tumors and draining lymph nodes, highlighting a mechanism whereby tumor-experienced effector T cells may mediate antitumor immunity at metastatic sites. Thus, our results provide insights into migration and function of tumor-infiltrating immune cells and the role of these cells in tumor immunity outside of primary tumor deposits.

tumor infiltrating | antitumor immune response | T cell | migration | immunotherapy

Antibody-based strategies to activate antitumor immunity (e.g., checkpoint inhibitors) are one of the recent successes in treatment of metastatic disease (1, 2). Furthermore, combining local radiotherapy of a single tumor with systemic treatment with checkpoint inhibitors is a potentially promising strategy to treat metastases (3). In this setting, it is important that tumor-experienced immune cells migrate out of primary tumor deposits to infiltrate tumors at distant sites and also to secondary lymphoid organs where antitumor responses are mounted. However, little is known about the nature of immune cell egress from primary tumors, largely due to the fact that until recently it has been impossible to distinguish tumor-egressing cells from all other immune cells. Thus, being able to identify recent tumor emigrants would provide important insight into migration and function of tumor-experienced cells.

Tumor-infiltrating immune cells can play opposing roles in tumor immunity, either promoting tumor rejection by direct tumor cell killing and stimulation of intratumor inflammatory responses or conversely, suppressing antitumor responses (4). Among tumor-infiltrating cells, the role of T cells is particularly complex, given the diversity of tumor-infiltrating T-cell subsets. Some T-cell subsets, including effector CD8<sup>+</sup> T cells and CD4<sup>+</sup> Th1 cells, promote tumor destruction through direct killing of tumor cells as well as production of antitumor cytokines such as IFN- $\gamma$

(5, 6). In contrast, T-cell subsets such as regulatory T (Treg) cells inhibit antitumor responses (7). The role of other T cells, such as  $\gamma\delta$  T cells, is less clear, as both pro- and antitumor effects have been attributed to these cells in different settings (4). The tumor microenvironment can alter the phenotype and function of tumor-infiltrating T cells, and their effect is not confined to primary tumor deposits. Therefore, the migration of immune cells out of the tumor has important clinical implications.

Here we used photoconvertible Kaede transgenic mice to track tumor-infiltrating immune cells as they leave tumors, thereby allowing us to obtain unique insights into their role outside primary tumor deposits. Unexpectedly, even though myeloid cells were the major infiltrating population, T cells were the major immune subset to exit tumors. Tumor-egressing T cells had a distinct composition from tumor-infiltrating and lymph node T cells and were made up of cells belonging to both  $\alpha\beta$  and  $\gamma\delta$  T-cell lineages, with active effector function consistent with a role for them in antitumor immunity. Furthermore, tumor-egressing T cells disseminated to distant tumors and draining lymph nodes, indicating a potential role for mediating antitumor responses at sites of metastasis.

## Results and Discussion

**Immune Cells Leave Primary Tumors and Accumulate in Draining Lymph Nodes.** Although immune infiltration of solid tumors has been extensively studied, the fate of immune cells once inside solid tumors remains unexplored. To understand the fate of

### Significance

Understanding the consequences of immune infiltration of solid tumors is vital to continued development of successful immune therapies. However, little is known about the fate of tumor-experienced leukocytes. Here we used in vivo photoconversion to label tumor-infiltrating cells and demonstrated specific egress and dissemination of effector T-cell subsets from tumors. The identity and functions of tumor-egressing cells, and those retained inside tumors, are of great importance to our understanding of tumor immunity because of the crucial role tumor-infiltrating cells play in primary tumors and their potential to provide antitumor immunity at secondary tumor sites and in secondary lymphoid organs. The results of this study will guide strategies that harness T-cell immunity for anticancer therapies.

Author contributions: T.T., H.R.H., R.B., and T.C. designed research; T.T., H.R.H., and J.B. performed research; M.T. contributed new reagents/analytic tools; T.T., H.R.H., J.B., and T.C. analyzed data; and T.T. and T.C. wrote the paper.

The authors declare no conflict of interest.

This article is a PNAS Direct Submission.

Freely available online through the PNAS open access option.

<sup>1</sup>To whom correspondence should be addressed. Email: t.chtanova@garvan.org.au.

This article contains supporting information online at [www.pnas.org/lookup/suppl/doi:10.1073/pnas.1618446114/-DCSupplemental](http://www.pnas.org/lookup/suppl/doi:10.1073/pnas.1618446114/-DCSupplemental).

tumor-infiltrating immune cells, we induced primary tumors by injecting widely used syngeneic Lewis lung carcinoma (LLC) cells into the ear pinnae of C57BL/6J mice. Flow cytometric analysis of tumors revealed that myeloid cells, including macrophages, neutrophils, and dendritic cells (DCs), made up the majority of tumor-infiltrating cells, whereas lymphocytes made up a much smaller fraction of the immune infiltrate (Fig. 1A).

To track the migration of tumor-conditioned immune cell subsets, we established a system that allows us to label tumor-infiltrating

cells without disruption to tumor integrity (Fig. 1B). This model makes use of a reporter mouse ubiquitously expressing the coral-derived, photoconvertible, fluorescent protein Kaede (8), which can be photoconverted from green to red after exposure to UV or violet light. As demonstrated by us (9, 10) and others (8), photoconvertible transgenic mice can be used to monitor cellular movement between organs and therefore represent a unique and powerful tool for labeling and tracking migratory tumor-infiltrating cells. LLC cells were injected into the ear pinnae of Kaede transgenic mice, leading to growth of tumor deposits that are readily accessible, without the need for inflammation-inducing surgical procedures. Once the tumors reached  $\sim 14 \text{ mm}^3$ , they were photoconverted by a brief exposure to white light from a cold light source (11). This approach allowed us to label cells  $\sim 2 \text{ mm}$  deep into the tumor ( $\sim 60\text{--}100\%$  of tumor depth) (Fig. 1C). Analysis of tumors immediately following photoconversion showed that the majority of tumor-infiltrating cells can be photoconverted using this approach (Fig. 1D). Furthermore, we observed photoconversion of all major tumor-infiltrating immune subsets (Fig. S1).

To track the fate of tumor-infiltrating cells, tumors were photoconverted and the mice were killed 24 h later for detection of photoconverted cells in various organs by flow cytometry. At this point, a substantial number of tumor-egressing photoconverted cells could be detected only in draining lymph nodes of photoconverted tumor-bearing mice and not in other organs (Fig. 1E). Indeed, the number of egressing cells found in the draining lymph nodes following tumor photoconversion was more than 10-fold greater than following photoconversion of resting ear skin (Fig. S2A).

To identify the route of immune cell migration from tumors to lymph nodes, we used two-photon microscopy to visualize LYVE-1-labeled lymphatic vessels in the skin surrounding photoconverted tumors. Using this approach, we detected photoconverted cells migrating inside lymphatic vessels (Fig. S3A). Furthermore, when we analyzed tumor-draining lymph nodes 4 h after photoconversion, we observed that most of the photoconverted cells were in or near the subcapsular sinus (Fig. S3B), where afferent lymph enters the tissue. Taken together, these results indicate that most tumor-egressing cells enter draining lymph nodes via afferent lymphatic vessels.

Upon detailed analysis, the majority of the photoconverted (tumor egressing) cells were found to be lymphocytes (Fig. 1F), rather than the myeloid cells that made up the majority of infiltrating cells within primary tumors (Fig. 1A). Notably,  $\text{CD3}^+$  T cells made up almost half (44%) of all tumor-egressing cells detected in draining lymph nodes. Similar findings were obtained in the widely used B16F10 melanoma model where again T cells made up the main tumor-egressing population (Fig. S4). The reason for this selective egress of immune cells is unclear but could be due to relatively rapid recirculation of T cells compared with myeloid subsets. The tumor microenvironment may also favor retention of some myeloid subsets. In an earlier study, we noted that inflammatory signals induced during sterile inflammation (of which tumors are a subset) are less likely to promote migration of some myeloid cells such as neutrophils (9). Notably, we also observed a substantial proportion of DCs among tumor-egressing cells (Fig. 1F), indicating a role for these cells in tumor antigen transport to secondary lymphoid organs.

Quantitation of photoconverted T cells in tumors and draining lymph nodes revealed that 24 h after photoconversion, a substantial proportion of photoconverted T cells ( $>20\%$ ) was found in tumor-draining lymph nodes (Fig. S5A). We next analyzed the kinetics of photoconverted T-cell migration from tumors to draining lymph nodes. The proportion of photoconverted T cells in tumors declined by 27% in the first 24 h (Fig. S5B) and then decreased more gradually over the next 48 h. Furthermore, tumor-egressing T cells could be detected in draining lymph

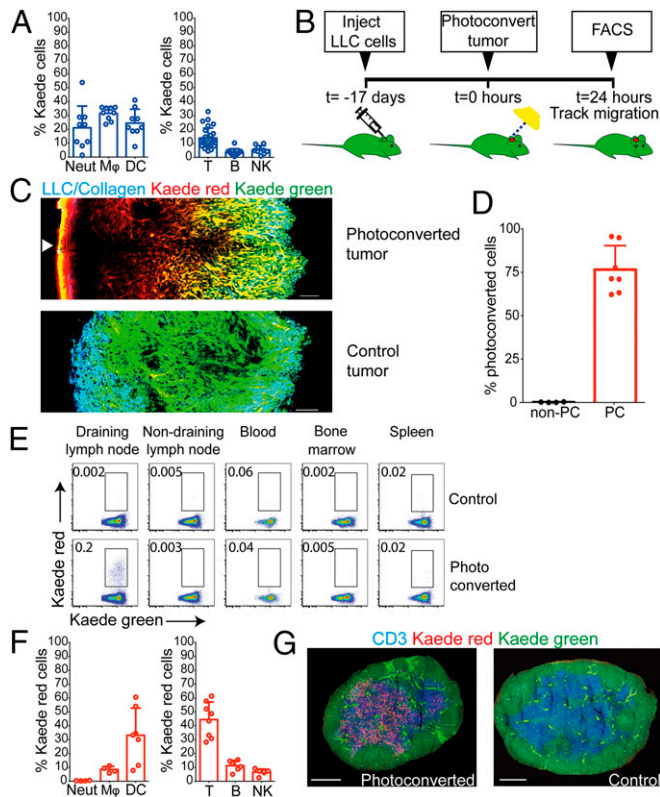


**Fig. 1.** T cells comprise the main tumor-egressing population and accumulate in draining lymph nodes. (A) Proportions of myeloid (Left) and lymphoid (Right) cells out of total Kaede cells infiltrating LLC ear tumors. Immune subsets are identified as follows: neutrophils,  $\text{Ly6G}^+\text{CD11b}^+$ ; macrophages,  $\text{Ly6G}^-\text{CD11b}^+$ ; DCs,  $\text{Ly6G}^-\text{CD11c}^+$ ; T cells,  $\text{CD3}^+$ ; B cells,  $\text{B220}^+$ ; and NK cells,  $\text{CD3}^-\text{NK1.1}^+$ . (B) Experimental setup for the detection of tumor-egressing cells. The  $2 \times 10^5$  LLC cells were inoculated into the ears of Kaede reporter mice. When the tumors reached  $14 \text{ mm}^3$  they were photoconverted by exposure to violet light for 20 min. Mice were killed 24 h later, and photoconverted cells were detected by flow cytometry. (C) Two-photon cross-section of a photoconverted and a control LLC tumor immediately after photoconversion. Arrow indicates the direction of photoconverting light. Photoconverted, red; unphotoconverted, green; and LLC/collagen, blue. (Scale bar,  $200 \mu\text{m}$ .) (D) Flow cytometric analysis of tumors immediately after photoconversion. (E) Analysis of photoconverted (PC) tumor-egressing cells after mice were treated as described in B. FACS profiles are representative of at least three independent experiments and are gated on total Kaede cells. (F) Proportions of myeloid (Left) and lymphoid (Right) cells out of photoconverted tumor-egressing Kaede cells in tumor-draining lymph nodes 24 h after photoconversion. Immune subsets are identified as in A. (G) Frozen sections of a tumor-draining lymph node 24 h after tumor photoconversion and a nonphotoconverted tumor-draining lymph node stained with anti-CD3 (blue). Kaede photoconverted cells (red) and nonphotoconverted Kaede cells (green) were visualized using confocal microscopy. (Scale bar,  $500 \mu\text{m}$ .) Sections are representative of at least three independent experiments. Each circle in A, D, and F represents a single tumor or lymph node. Data shown as mean + SD were pooled from at least two independent experiments with at least two mice per group (A, D, and F).

nodes as early as 4 h after photoconversion (Fig. S5C). Their proportion in draining lymph nodes increased rapidly, peaked by 24 h, and declined only slightly over the next 48 h (partly due to the influx of nonphotoconverted cells into tumors and lymph nodes as well as gradual loss of photoconverted protein at longer time points). Thus, photoconverted T cells rapidly egressed tumors and migrated to draining lymph nodes and most of this emigration occurred in the first 24 h.

We next examined the localization of tumor-egressing cells in frozen sections of draining lymph nodes of Kaede transgenic mice harvested 24 h after photoconversion. By this time, most of the photoconverted cells were located in the lymph node paracortex, consistent with their being mostly T cells and dendritic cells (Fig. 1G).

**Characterization of Tumor-Egressing T Cells.** The next step was to identify the T-cell subsets that emigrate from primary tumors to draining lymph nodes. Analysis of draining lymph nodes 24 h after tumor photoconversion revealed that both CD4<sup>+</sup> and CD8<sup>+</sup> T cells left the primary tumor site (Fig. 2A). However, the proportions of CD4<sup>+</sup> and CD8<sup>+</sup> T cells among tumor-egressing T cells were decreased compared with CD4<sup>+</sup> and CD8<sup>+</sup> T-cell proportions among total lymph node T cells (Fig. 2B). In addition to CD4<sup>+</sup> and CD8<sup>+</sup> T cells, the photoconverted T-cell population also contained a large proportion of CD4<sup>-</sup>CD8<sup>-</sup> [double negative (DN)] T cells. The proportion of DN T cells in the tumor-egressing population was increased more than sevenfold compared with the proportion of these cells among total lymph node T cells (Fig. 2B). When we compared the proportions of T-cell subsets inside primary tumors with those that had migrated to draining lymph nodes in the 24 h following photoconversion (Fig. 2B), the proportion of conventional single positive CD8<sup>+</sup> T cells (and to a lesser extent CD4<sup>+</sup>) emigrating from tumors was increased compared with the corresponding subset within tumor deposits, whereas the inverse was true for DN T cells. Thus, the enrichment in DN T cells among tumor-egressing cells reflects their relative abundance in the tumor deposit, rather than preferential egress from tumors. Therefore,

our results suggest that DN T cells were retained in the tumor for longer periods of time than CD4<sup>+</sup> and CD8<sup>+</sup> T cells, which appeared to egress from the tumor more rapidly. This difference in migratory capacity may relate to the ability of CD8<sup>+</sup> T cells to recirculate between inflamed tissues and secondary lymphoid organs (12, 13) but may also be due to signals within the tumor microenvironment selectively retaining some T-cell subsets. Thus, our results suggest that T-cell egress from tumors is selectively regulated.

We noted earlier that the number of tumor-egressing cells in the draining lymph nodes following tumor photoconversion was more than 10-fold greater than following photoconversion of resting ear skin (Fig. S2A). We next examined whether proportions of T-cell subsets egressing from tumors differed from those of T cells emigrating from resting skin (Fig. S2B). The tumor-egressing T-cell population was enriched in DN T cells but had fewer CD4<sup>+</sup> T cells compared with T-cell subsets that migrated from resting skin to draining lymph nodes in unmanipulated Kaede transgenic mice. Thus, the tumor-egressing T-cell population has a distinct composition from T cells migrating to lymph nodes from surrounding tissue.

**Effector T Cells Comprise the Majority of Tumor-Egressing T Cells.** To distinguish between naïve, central memory (CM), and effector memory (EM) subsets, we stained tumor-draining lymph nodes in photoconverted mice with antibodies against CD44 and CD62L. Analysis of draining lymph nodes showed that a high proportion of tumor-egressing CD4<sup>+</sup> and CD8<sup>+</sup> T cells was either of effector and/or central memory phenotype (Fig. 3A and B). This observation reflects the memory phenotype of the CD4<sup>+</sup> and CD8<sup>+</sup> T cells present within the LLC tumors.

We next examined the expression of cell surface markers indicative of T-cell activation and noted that a significantly higher proportion of tumor-egressing cells was positive for T-cell activation markers CD69 as well as CD25 (Fig. 3C) compared with total lymph node T cells (consistent with the activation profile of tumor-infiltrating T cells). Because CD25 is also expressed by Treg cells, we used additional markers to determine whether CD25<sup>+</sup>CD4<sup>+</sup> T cells are activated effector or Treg cells. To date, the best way to identify Treg cells is via the expression of Treg-specific transcription factor Foxp3. However, the staining protocol required to detect intracellular Foxp3 destroys the fluorescent signal of Kaede protein, which meant that we had to use an alternative Treg cell surface marker (FR4) to determine whether CD25<sup>+</sup> T cells were in fact Treg cells (14). In our hands, FR4 was expressed on >90% of Foxp3<sup>+</sup> lymph node T cells (Fig. S6), providing a reliable way to identify Treg cells. Staining for FR4 revealed that >80% of total lymph node CD4<sup>+</sup>CD25<sup>+</sup> T cells expressed this marker, suggesting that the majority of lymph node CD4<sup>+</sup>CD25<sup>+</sup> cells were indeed Treg cells (Fig. 3D, Left). However, a much smaller proportion of tumor-egressing CD4<sup>+</sup>CD25<sup>+</sup> T cells (34%) expressed FR4 (Fig. 3D, Left). Consistent with this finding, only a small proportion (~11%) of tumor-egressing CD4<sup>+</sup> T cells was FR4<sup>+</sup>CD25<sup>+</sup> and this was similar to total lymph node CD4<sup>+</sup> T cells (Fig. 3D, Right). Thus, our results suggest that the majority of tumor-conditioned T cells in draining lymph nodes have an effector rather than regulatory phenotype.

We also noted that tumor-infiltrating CD4<sup>+</sup> and DN T cells contained a higher proportion of T cells coexpressing PD-1 and Tim-3 compared with T cells that exited the tumor (Fig. 3E). Exhaustion, characterized by hyporesponsiveness to reactivation, poor effector functions, and up-regulation of inhibitory markers such as PD-1 and Tim-3, frequently affects tumor-infiltrating T cells in solid tumors (15). The precise phenotype that accompanies exhaustion in CD4<sup>+</sup> T cells is not well understood, although it is thought that at least some exhausted CD4<sup>+</sup> T cells express the same markers as exhausted CD8<sup>+</sup> T cells (15). Thus,

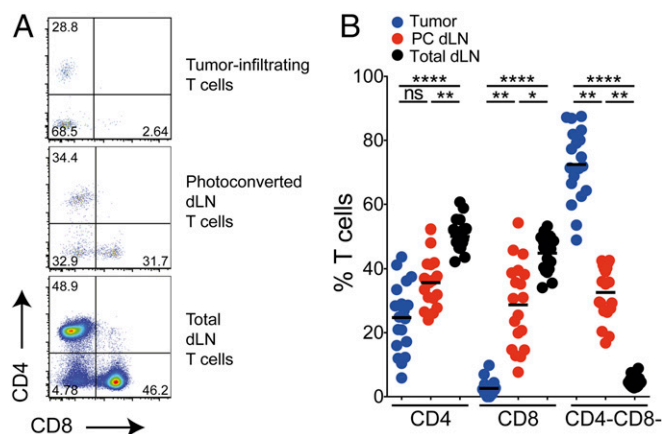


**Fig. 2.** Tumor-egressing T-cell subsets. (A) Flow cytometry profiles of tumor-infiltrating, photoconverted draining lymph node and total draining lymph node CD3<sup>+</sup> T-cell subsets analyzed 24 h after tumor photoconversion. Profiles are representative of at least three independent experiments. (B) Analysis of tumor-infiltrating (blue), photoconverted draining lymph node (red), and total draining lymph node (black) CD3<sup>+</sup> T-cell subsets 24 h after photoconversion. Each circle represents a single lymph node or tumor. Data shown as mean were pooled from at least six independent experiments with at least three mice per group and analyzed using a Friedman test. ns, not significant; \**P* < 0.05, \*\**P* < 0.01, \*\*\*\**P* < 0.0001. PC, photoconverted; dLN, draining lymph node.

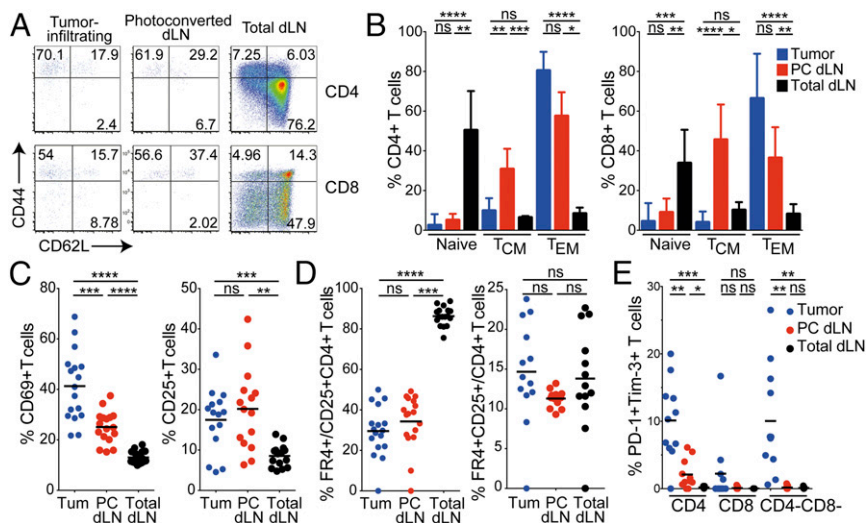


**Fig. 3.** Tumor-egressing T cells possess activated and effector/memory phenotypes. (A) Flow cytometry profiles of tumor-infiltrating, photoconverted draining lymph node and total draining lymph node CD4<sup>+</sup> and CD8<sup>+</sup> T-cell subsets. Profiles are representative of at least three independent experiments. (B) Proportions of naive (CD44<sup>+</sup>CD62L<sup>+</sup>), central (CD44<sup>+</sup>CD62L<sup>+</sup>), and effector (CD44<sup>+</sup>CD62L<sup>-</sup>) memory T cells among tumor-infiltrating (blue), photoconverted draining lymph node (red), and total (black) lymph node CD4<sup>+</sup> and CD8<sup>+</sup> T-cell subsets. (C) Proportions of CD69<sup>+</sup> (Left) and CD25<sup>+</sup> (Right) CD3<sup>+</sup> T cells among tumor-infiltrating (blue), photoconverted draining lymph node (red), and total draining lymph node (black) T cells. (D) Proportions of FR4<sup>+</sup> out of CD25<sup>+</sup>CD4<sup>+</sup> T cells (Left) and proportions of FR4<sup>+</sup>CD25<sup>+</sup> out of CD4<sup>+</sup> T cells (Right) out of tumor-infiltrating (blue), photoconverted draining lymph node (red), and total draining lymph node (black) T cells. (E) Proportions of tumor-infiltrating (blue), photoconverted draining lymph node (red), and total draining lymph node PD-1<sup>+</sup>Tim-3<sup>+</sup>CD3<sup>+</sup> T-cell subsets. Data shown as mean (C–E) + SD (B) were analyzed using a Wilcoxon matched-pairs signed rank test (B), a repeated measures (RM) one-way ANOVA test (C and D, Right and E) or a Friedman test (D, Left). ns, not significant; \**P* < 0.05, \*\**P* < 0.01, \*\*\**P* < 0.001, \*\*\*\**P* < 0.0001. Each circle represents a single tumor or lymph node analyzed 24 h after tumor photoconversion. Data in B–E were pooled from at least three independent experiments with at least three mice per group. PC, photoconverted; dLN, draining lymph node.

it is possible that PD-1<sup>+</sup>Tim-3<sup>+</sup>CD4<sup>+</sup> T cells were preferentially retained in tumors due to the impaired ability of exhausted cells to respond to chemotactic signals and egress from tumors. Alternatively, CD4<sup>+</sup> and DN T cells could down-modulate these cell surface markers upon egress from tumors. Furthermore, PD-1 is also expressed on activated T cells and therefore may indicate selective retention of T cells that have recently undergone antigen-specific activation.

**Molecular Mechanism of T-Cell Egress from Tumors.** To investigate the molecular mechanisms of T-cell emigration from tumors to draining lymph nodes, we first administered pertussis toxin to block G protein-coupled receptor signaling. Our analysis revealed that egress was significantly reduced after inhibitor administration, indicating that migration from tumors is dependent on G protein-coupled receptors (Fig. S7A). We next tested the role of chemokine receptor CCR7, which has been implicated in immune cell entry into lymph nodes (16). Our results show that T-cell migration was independent of CCR7 (Fig. S7B). This observation is in line with the finding that tumor-egressing T cells possess a mostly effector/memory phenotype (Fig. 3B) and therefore may be less reliant on CCR7 for lymph node entry than naive T cells (17). It is possible that other chemokine receptors expressed on effector T cells, such as CXCR3, CXCR4, and CCR6, guide migration from tumors.

**$\gamma\delta$  T Cells Are Enriched Among Tumor-Egressing Cells in Lymph Nodes.** Closer examination of the tumor-egressing DN subset revealed that more than half expressed  $\gamma\delta$  T-cell receptors (TCRs) (Fig. 4A). Strikingly,  $\gamma\delta$  T cells were enriched 11-fold among tumor-egressing T cells compared with the proportion present among total lymph node T cells (Fig. 4B), suggesting that  $\gamma\delta$  T cells may play a unique function in tumor immune responses. The enrichment in  $\gamma\delta$  T cells compared with  $\alpha\beta$  T cells may be due to the location of the tumor near the  $\gamma\delta$  T-cell-rich environment of the skin. However, it is still unclear how much influence the resident

immune population of the tissue where the primary tumor is located has on the make up of tumor-egressing immune subsets.

To explore the phenotype of tumor-egressing  $\gamma\delta$  T cells, we analyzed them for expression of V $\gamma$ 1, V $\gamma$ 4, and V $\gamma$ 5 chains (according to nomenclature in ref. 18) known to be present on  $\gamma\delta$  T-cell subsets in skin and/or lymph nodes (19–21). Based on TCR use, the V $\gamma$ 4 subset was the predominant population among tumor-egressing  $\gamma\delta$  T cells (Fig. 4C). This finding is in contrast to V $\gamma$  expression among tumor-infiltrating cells where the V $\gamma$ 1 subset predominated, suggesting that, consistent with previous reports (22), V $\gamma$ 4<sup>+</sup> T cells have a greater migratory potential. The V $\gamma$ 4 subset among tumor-egressing  $\gamma\delta$  T cells was also significantly enriched relative to lymph node  $\gamma\delta$  T-cell subsets (Fig. 4C).

We then investigated expression of the costimulatory molecule CD27, which can enhance T-cell expression of IFN- $\gamma$  and suppress IL-17 production (23). Tumor-egressing  $\gamma\delta$  T cells had a lower proportion of CD27<sup>+</sup>  $\gamma\delta$  T cells compared with their lymph node counterparts (Fig. 4D). CD27 can also down-modulate the chemokine receptor CCR6, which is expressed by IL-17-producing T-cell subsets, including  $\gamma\delta$  T cells (24). Consistent with decreased proportions of CD27<sup>+</sup> cells, we found that CCR6 expression was enhanced on tumor-egressing  $\gamma\delta$  T cells compared with total lymph node  $\gamma\delta$  T cells (Fig. 4E). Similarly, we observed increased expression of  $\alpha$ E integrin CD103 on tumor-egressing  $\gamma\delta$  T cells (Fig. 4F), a molecule previously associated with IL-17-producing  $\gamma\delta$  T-cell subsets (25). Thus, tumor-egressing  $\gamma\delta$  T cells possess a phenotype consistent with IL-17 production.

**Dissemination and Function of Tumor-Egressing T Cells.** The phenotype of tumor-egressing T cells suggests that they may possess enhanced effector functions. We therefore first examined whether the expression IFN- $\gamma$ , which plays a critical role in antitumor defense (5, 26), is augmented in any of the tumor-egressing T-cell subsets (Fig. 5A). The intracellular staining protocol commonly

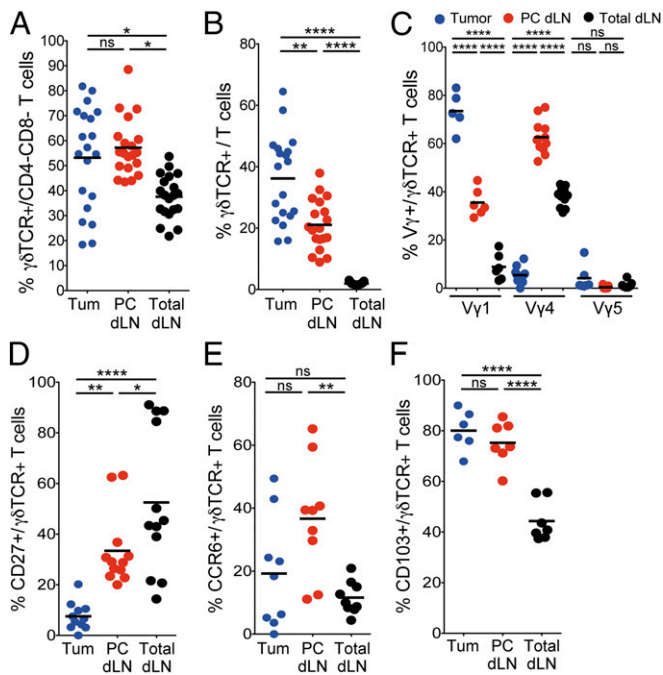


**Fig. 4.** Identity of tumor-egressing  $\gamma\delta$  T cells.  $\gamma\delta$  T-cell proportion among tumor-infiltrating (blue), photoconverted draining lymph node (red), and total draining lymph node (black) CD4<sup>-</sup>CD8<sup>-</sup>CD3<sup>+</sup> T cells (A) and CD3<sup>+</sup> T cells (B). (C) Proportions of tumor-infiltrating (blue), photoconverted draining lymph node (red), and total draining lymph node (black)  $\gamma\delta$  T-cell subsets. Proportions of CD27<sup>+</sup> (D), CCR6<sup>+</sup> (E), and CD103<sup>+</sup> (F)  $\gamma\delta$  T cells out of tumor-infiltrating (blue), photoconverted draining lymph node (red), and total draining lymph node (black)  $\gamma\delta$  T cells. Data shown as mean were analyzed using a Friedman test (A), a RM one-way ANOVA test (B and E), or an ordinary one-way ANOVA test (C, D, and F). ns, not significant; \* $P < 0.05$ , \*\* $P < 0.01$ , \*\*\*\* $P < 0.0001$ . All data were analyzed 24 h after tumor photoconversion and pooled from at least two independent experiments with at least two mice per group. Each circle represents a single tumor or lymph node. PC, photoconverted; dLN, draining lymph node.

used to examine cytokine production leads to a decrease in fluorescence of photoconverted cells, making them difficult to detect. To circumvent this possibility, we sorted photoconverted and nonphotoconverted cells and conducted assays on sorted populations to detect cytokines secreted into the culture media. Photoconverted CD4<sup>+</sup> and especially CD8<sup>+</sup> T cells showed enhanced IFN- $\gamma$  production in comparison with nonphotoconverted CD4<sup>+</sup> and CD8<sup>+</sup> T cells. In contrast, there was a decrease in IFN- $\gamma$  levels in tumor-egressing (Fig. 5A) as well as in tumor-infiltrating (Fig. S8)  $\gamma\delta$  T cells compared with nonphotoconverted lymph node  $\gamma\delta$  T cells.

We next assessed the expression of IL-17 by tumor-egressing T cells, because this cytokine has also been implicated in tumor immunity (27). Analysis of IL-17 showed that tumor-egressing  $\gamma\delta$  T cells preferentially expressed IL-17A compared with total lymph node  $\gamma\delta$  T cells (Fig. 5B). This finding is consistent with an increase in the proportion of CD27<sup>-</sup> and CCR6<sup>+</sup> subsets among the tumor-egressing  $\gamma\delta$  T cells (Fig. 4D and E), both of which have been linked with IL-17 production (28). Tumor-egressing  $\alpha\beta$  T cells also showed enhanced expression of IL-17 compared with lymph node T cells, although relatively few of them produced IL-17 in comparison with  $\gamma\delta$  T cells. Notably,  $\gamma\delta$ -derived IL-17 can enhance recruitment of CD8<sup>+</sup> T-cell subsets (29) but can also promote tumor angiogenesis and recruitment of myeloid-derived suppressor cells (30) as well as tumor metastasis (31).

To test whether cytotoxic function is augmented in tumor-egressing T cells, we analyzed cell surface expression of CD107a,

a marker of degranulation and cytotoxicity (32). We found that photoconverted tumor-egressing T cells had significantly higher expression of CD107a compared with nonphotoconverted T cells in the draining lymph node (Fig. 5C). This finding was true for both subsets of  $\alpha\beta$  T cells but not for  $\gamma\delta$  T cells. Thus, our results indicate that tumor-egressing T cells are a heterogeneous population of antigen-experienced cells that are primed for effector functions. Whereas tumor-egressing  $\alpha\beta$  T cells appear to have antitumor functions characterized by the expression of IFN- $\gamma$  and CD107a, the role of tumor-egressing  $\gamma\delta$  T cells is less clear, as they have been implicated in pro- and antitumor responses (4). However, the relative enrichment of this subset among tumor-egressing T cells together with their capacity for rapid cytokine production make  $\gamma\delta$  T cells an attractive target for immune-based cancer therapies.

Tumor-infiltrating T cells play a crucial role in primary tumors but also have the potential to provide antitumor immunity at secondary tumor sites. Therefore, we examined intratumoral T-cell dissemination in the presence of a secondary tumor. Photoconvertible transgenic mice were inoculated with LLC tumor cells in both ears. Once tumors developed on both sides, we photoconverted one of the tumors and examined whether tumor-egressing T cells can migrate to distal lymph nodes and tumor deposits. Analysis of draining, semidrainage, nondraining, and contralateral draining lymph nodes (draining the nonphotoconverted tumor) over a period of 72 h, showed that, as expected, tumor-draining lymph nodes contained the highest number of tumor-egressing

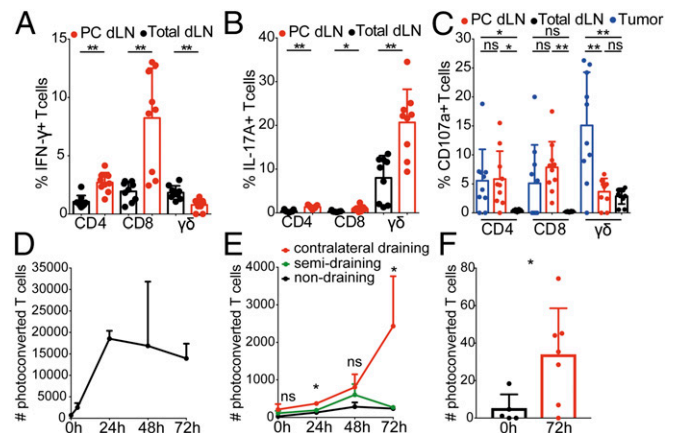


**Fig. 5.** Effector function and dissemination of tumor-egressing T cells. Proportions of (A) IFN- $\gamma$ <sup>+</sup> and (B) IL-17A<sup>+</sup> CD3<sup>+</sup> T cells among total (black) and photoconverted (red) lymph node T-cell subsets 24 h after tumor photoconversion. Photoconverted and nonphotoconverted CD4<sup>+</sup>, CD8<sup>+</sup>, and  $\gamma\delta$  CD3<sup>+</sup> T cells were sorted and stimulated overnight with phorbol myristate acetate (PMA)/ionomycin. (C) CD107a expression on tumor-infiltrating (blue), photoconverted draining lymph node (red), and total draining lymph node (black) CD3<sup>+</sup> T-cell subsets 24 h after tumor photoconversion. Photoconverted CD3<sup>+</sup> T-cell number 4 h (D) and immediately after (0 h) and 24, 48, and 72 h (D and E) after photoconversion in photoconverted tumor-draining lymph nodes (D) and in contralateral draining, semidrainage, and nondraining lymph nodes (E). (F) Photoconverted CD3<sup>+</sup> T-cell number immediately after and 72 h after photoconversion in contralateral nonphotoconverted tumors. Data shown as mean + SD (A–C and F) or + SEM (D and E) were analyzed using a Wilcoxon matched-pairs signed rank test (A and B), a RM one-way ANOVA test (C), a Kruskal–Wallis test (E), or a Mann–Whitney test (F).  $P$  values in E indicate comparisons of semidrainage or nondraining lymph nodes to contralateral draining lymph nodes. ns, not significant; \* $P < 0.05$ , \*\* $P < 0.01$ . All data were pooled from at least three independent experiments with at least two mice per group. Each circle in A and B represents at least four pooled draining lymph nodes. Each time point in D and E represents at least four lymph nodes. PC, photoconverted; dLN, draining lymph node.

T cells (Fig. 5D). Notably, contralateral tumor-draining lymph nodes contained the next highest number of tumor-egressing T cells, and this number was significantly higher than the number of photoconverted T cells in all other lymph nodes (Fig. 5E), suggesting that tumor-experienced effector T cells are selectively recruited to this site. Furthermore, we observed a significant increase in the number of photoconverted T cells in contralateral nonphotoconverted tumors 72 h after photoconversion (Fig. 5F), indicating that intratumoral T cells can disseminate to distant tumors. Migration of tumor-experienced cells to these sites could be a part of an immune surveillance program that allows anti-tumor effector T cells to patrol sites of metastasis. Notably, radiation of a single tumor enhances the activity of tumor-infiltrating T cells and can also lead to eradication of distal tumors potentially via migration of tumor-experienced effector T cells (33). Therefore, our findings could have important implications for the development of novel approaches to treat metastases that rely on abscopal effects of localized tumor cell killing by radiation in combination with systemic activation of antitumor immunity by checkpoint inhibitors (3). Thus, enhanced emigration of tumor-experienced effector T cells from primary tumors could promote more effective systemic immunity and antitumor responses at secondary tumor sites.

In summary, here we identified tumor-experienced immune cells that can egress primary tumors as well as cells that are retained inside tumor deposits, highlighting selective regulation of dissemination of tumor-conditioned immune cells. This work sheds light on the roles of tumor-infiltrating immune cells

in tumor immunity outside primary tumors and may provide additional therapeutic opportunities for controlling immune responses at distal sites such as secondary metastatic tumors and in draining lymph nodes where antitumor responses are initiated.

## Materials and Methods

More detailed information is provided in *SI Materials and Methods*. The experimental protocols were approved by the Garvan Institute of Medical Research/St. Vincent's Hospital Animal Ethics Committee.

Tumor cells were cultured for less than 4 wk in 10% FBS DMEM supplemented with 2 mM L-glutamine, 50 units/mL penicillin, and 50  $\mu$ g/mL streptomycin, harvested in logarithmic growth (75–90% confluence). Mouse ear pinnae were injected with  $2 \times 10^5$  tumor cells (in a volume of 5  $\mu$ L) using a 10- $\mu$ L Hamilton syringe with 30-gauge needle. Once ear tumors reached an average volume of 14 mm<sup>3</sup>, they were photoconverted to label tumor-infiltrating cells. Ear skin around the tumor was protected with a surgical cloth to avoid photoconversion of surrounding tissue, and tumors were irradiated for 20 min with violet light from a cold-light source fitted with a conversion filter (Zeiss) to minimize phototoxicity. Resting ears were photoconverted for 20 min using the same approach. Photoconverted Kaede red cells were detected by both flow cytometry and fluorescence microscopy 24 h after photoconversion.

**ACKNOWLEDGMENTS.** We thank Profs. Anthony Basten, Christopher Goodnow, and Charles Mackay and Drs. Jessica Stolp and Kylie Webster for scientific discussion and critical reading of the manuscript. This research was funded by the Human Frontier Science Program, National Health and Medical Research Council Project Grant GNT1106043 (to T.C.), a University of New South Wales International Postgraduate Award (to T.T.), and Peter and Val Duncan.

- Pardoll DM (2012) The blockade of immune checkpoints in cancer immunotherapy. *Nat Rev Cancer* 12:252–264.
- Nishikawa H, Sakaguchi S (2014) Regulatory T cells in cancer immunotherapy. *Curr Opin Immunol* 27:1–7.
- Twyman-Saint Victor C, et al. (2015) Radiation and dual checkpoint blockade activate non-redundant immune mechanisms in cancer. *Nature* 520:373–377.
- Lança T, Silva-Santos B (2012) The split nature of tumor-infiltrating leukocytes: Implications for cancer surveillance and immunotherapy. *Oncol Immunology* 1:717–725.
- Shankaran V, et al. (2001) IFN $\gamma$  and lymphocytes prevent primary tumour development and shape tumour immunogenicity. *Nature* 410:1107–1111.
- Hishii M, Kurnick JT, Ramirez-Montagut T, Pandolfi F (1999) Studies of the mechanism of cytotoxicity by tumour-infiltrating lymphocytes. *Clin Exp Immunol* 116:388–394.
- Josefowicz SZ, Lu LF, Rudensky AY (2012) Regulatory T cells: Mechanisms of differentiation and function. *Annu Rev Immunol* 30:531–564.
- Tomura M, et al. (2008) Monitoring cellular movement in vivo with photoconvertible fluorescence protein “Kaede” transgenic mice. *Proc Natl Acad Sci USA* 105:10871–10876.
- Hampton HR, Bailey J, Tomura M, Brink R, Chtanova T (2015) Microbe-dependent lymphatic migration of neutrophils modulates lymphocyte proliferation in lymph nodes. *Nat Commun* 6:7139.
- Suan D, et al. (2015) T follicular helper cells have distinct modes of migration and molecular signatures in naive and memory immune responses. *Immunity* 42:704–718.
- Chtanova T, et al. (2014) Real-time interactive two-photon photoconversion of recirculating lymphocytes for discontinuous cell tracking in live adult mice. *J Biophotonics* 7:425–433.
- Hickman HD, et al. (2011) Chemokines control naive CD8<sup>+</sup> T cell selection of optimal lymph node antigen presenting cells. *J Exp Med* 208:2511–2524.
- Castellino F, et al. (2006) Chemokines enhance immunity by guiding naive CD8<sup>+</sup> T cells to sites of CD4<sup>+</sup> T cell-dendritic cell interaction. *Nature* 440:890–895.
- Yamaguchi T, et al. (2007) Control of immune responses by antigen-specific regulatory T cells expressing the folate receptor. *Immunity* 27:145–159.
- Pauken KE, Wherry EJ (2015) Overcoming T cell exhaustion in infection and cancer. *Trends Immunol* 36:265–276.
- Förster R, et al. (1999) CCR7 coordinates the primary immune response by establishing functional microenvironments in secondary lymphoid organs. *Cell* 99:23–33.
- Guarda G, et al. (2007) L-selectin-negative CCR7<sup>+</sup> effector and memory CD8<sup>+</sup> T cells enter reactive lymph nodes and kill dendritic cells. *Nat Immunol* 8:743–752.
- Heilig JS, Tonegawa S (1986) Diversity of murine gamma genes and expression in fetal and adult T lymphocytes. *Nature* 322:836–840.
- Asarnow DM, et al. (1988) Limited diversity of gamma delta antigen receptor genes of Thy-1<sup>+</sup> dendritic epidermal cells. *Cell* 55:837–847.
- Cai Y, et al. (2011) Pivotal role of dermal IL-17-producing  $\gamma\delta$  T cells in skin inflammation. *Immunity* 35:596–610.
- Pereira P, Gerber D, Huang SY, Tonegawa S (1995) Ontogenic development and tissue distribution of V gamma 1-expressing gamma/delta T lymphocytes in normal mice. *J Exp Med* 182:1921–1930.
- Gray EE, Suzuki K, Cyster JG (2011) Cutting edge: Identification of a motile IL-17-producing gammadelta T cell population in the dermis. *J Immunol* 186:6091–6095.
- Coquet JM, et al. (2013) The CD27 and CD70 costimulatory pathway inhibits effector function of T helper 17 cells and attenuates associated autoimmunity. *Immunity* 38:53–65.
- Haas JD, et al. (2009) CCR6 and NK1.1 distinguish between IL-17A and IFN- $\gamma$ -producing gammadelta effector T cells. *Eur J Immunol* 39:3488–3497.
- Gray EE, et al. (2013) Deficiency in IL-17-committed V $\gamma$ 4(+)  $\gamma\delta$  T cells in a spontaneous Sox13-mutant CD45.1(+) congenic mouse strain provides protection from dermatitis. *Nat Immunol* 14:584–592.
- Sadanaga N, et al. (1999) Local secretion of IFN- $\gamma$  induces an antitumor response: Comparison between T cells plus IL-2 and IFN- $\gamma$ -transfected tumor cells. *J Immunother* 22:315–323.
- Murugaiyan G, Saha B (2009) Protumor vs antitumor functions of IL-17. *J Immunol* 183:4169–4175.
- Ribot JC, et al. (2009) CD27 is a thymic determinant of the balance between interferon- $\gamma$ - and interleukin 17-producing gammadelta T cell subsets. *Nat Immunol* 10:427–436.
- Ma Y, et al. (2011) Contribution of IL-17-producing gamma delta T cells to the efficacy of anticancer chemotherapy. *J Exp Med* 208:491–503.
- Rei M, et al. (2014) Murine CD27(–) V $\gamma$ 6(+)  $\gamma\delta$  T cells producing IL-17A promote ovarian cancer growth via mobilization of protumor small peritoneal macrophages. *Proc Natl Acad Sci USA* 111:E3562–E3570.
- Coffelt SB, et al. (2015) IL-17-producing  $\gamma\delta$  T cells and neutrophils conspire to promote breast cancer metastasis. *Nature* 522:345–348.
- Betts MR, et al. (2003) Sensitive and viable identification of antigen-specific CD8<sup>+</sup> T cells by a flow cytometric assay for degranulation. *J Immunol Methods* 281:65–78.
- Tang C, et al. (2014) Combining radiation and immunotherapy: A new systemic therapy for solid tumors? *Cancer Immunol Res* 2:831–838.